Polarization-dependent strong coupling in elliptical high-Q micropillar cavities

S. Reitzenstein,* C. Böckler, A. Löffler, S. Höfling, L. Worschech, and A. Forchel
Technische Physik, Physikalisches Institut, and Wilhelm Conrad Röntgen Research Center for Complex Material Systems, Universität Würzburg, Am Hubland, D-97074 Würzburg, Germany

P. Yao and S. Hughes
Department of Physics, Queen's University, Kingston, Ontario, Canada K7L 3N6
(Received 24 August 2010; published 10 December 2010)

We present a combined experimental and theoretical study of the polarization-dependent strong-coupling regime between two quantum dots and an asymmetric micropillar cavity. The photoluminescence emission demonstrates that the fundamental cavity mode is split into two linearly polarized cavity modes, both of which are coupled to 45%-aligned quantum dot excitons. We map out various single-exciton and double-exciton coupling regimes, including the full energy dispersion of dual-exciton and dual-cavity emission under x and y detection angle. To explain the complex light-matter coupling we apply an analytical photon Green function approach that successfully reproduces the qualitative features of our experimental data.

DOI: 10.1103/PhysRevB.82.235313 PACS number(s): 78.67.−n, 81.07.Ta, 42.50.Pq

I. INTRODUCTION

The coherent interaction of light and matter at the quantum limit presents a central topic in modern quantum optics. In recent years, a number of solid-state platforms have been established to realize the strong-coupling regime in the framework of cavity quantum electrodynamics (cQED). Particular attention has been paid to quantum-dot (QD)-microcavity systems with the prospect of compact implementations and scalability. Indeed, since the first observation of strong coupling in quantum-dot-microcavity systems,[1,2] enormous scientific effort has been directed to this field of semiconductor technology and important effects such as the quantum nature of strong coupling,[3,4] field quantization, and the Jaynes-Cummings ladder[5,6] as well as coherent coupling of QDs via a common cavity mode could be demonstrated.[7] More recently, the studies have also been extended to electrically contacted systems which is of high importance for practical device applications.[8–10]

Most of the aforementioned experiments can be explained by only accounting for the single polarization nature of the photonic cavity. However, the polarization states of the interaction modes also give access to important information of the underlying physics. For instance, polarization-resolved studies allow one to identify the charge state of the involved QD exciton lines.[11] Moreover, in magneto-optical studies it has been demonstrated that distinct polarization states of the photon and exciton states can lead to an effective photon-photon coupling mediated by the excitonic transition.[12] The fact that typical semiconductor cavities yield nondegenerate cavity modes is also useful for various quantum optical applications, including proposals for the creation of polarization-entangled photon pairs.[13,14] In order to exploit the dual coupling of excitons to orthogonal cavity modes, it is desirable to map out the strong-coupling regime as a function of polarization.

In this work, we present experimental and theoretical studies of polarization-resolved strong coupling between excitonic states of elongated $In_{0.3}Ga_{0.7}As$ QDs and linearly polarized components of the split fundamental mode of a micropillar cavity. Polarization-resolved photoluminescence (PL) spectra show pronounced asymmetries of the light-matter coupling strength depending on the orientation of the emitter dipole and the cavity-mode polarization. The experimental observations are in good agreement with our calculations based on a canonical Hamiltonian[15,16] and Green function approach, and show that the relative orientation and strength of the emitter dipoles and the cavity mode can be essential parameters in the strong-coupling regime. Exploiting cQED and nonlinearities in these semiconductor systems could pave the way to fast optical switching between an uncoupled system and a strongly coupled system under polarization-resolved excitation conditions.

Our paper is organized as follows. In Sec. II, we introduce the theoretical framework that allows us to analytically compute the PL. The theory is based on a photon Green function approach that exploits scattering theory and a canonical Hamiltonian to derive the electric-field operator for any general medium containing any finite number of QDs or dipoles; explicit solutions are obtained for two QDs coupled to two orthogonal cavity modes. In Sec. III, we describe the experiment and cavity-QD system under investigation that is based on a planar microcavity system containing large elongated QDs in the active region of the pillar. We then present measurements and simulations of the PL emission, focusing on the polarization dependence of the optical spectra. We briefly conclude in Sec. IV.

II. THEORY

Before showing the PL measurements, we first describe the theory that we use to compare with experimental data. We employ a canonical Hamiltonian that quantizes the macroscopic electromagnetic fields,[15,16] and use the dipole approximation for the QD-medium coupling. Labeling two *target* (possibly strongly coupled) QDs a and b, we obtain the multipolar-coupling Hamiltonian,

 ©2010 The American Physical Society

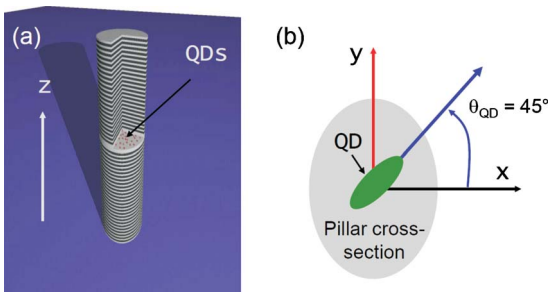

FIG. 1. (Color online) (a) Schematic of the micropillar system containing a layer of QDs in the active region. (b) For a target quantum dot, we show the dipole orientation of 45° with respect to the orthogonal cavity-mode directions, x and y. The system is incoherently exited and the emission PL is detected for any specific polarization direction. The pillar system is always slightly asymmetric which results in a frequency splitting of the fundamental cavity mode into well-defined x-polarized and y-polarized cavity modes, with separate cavity resonances ($\omega_{x/y}$) and linewidths ($\Gamma_{x/y}$).

$$\hat{H} = \sum_{m=a,b} \hbar\omega_m \hat{\sigma}_m^+ \hat{\sigma}_m^- + \sum_{\lambda} \hbar\omega_\lambda \hat{a}_\lambda^\dagger \hat{a}_\lambda - i\hbar \sum_{m=a,b;\lambda} (\hat{\sigma}_m^- + \hat{\sigma}_m^+) \times (g_{m\lambda}\hat{a}_\lambda - g_{m\lambda}^* \hat{a}_\lambda^\dagger), \tag{1}$$

where $\hat{a}_\lambda$ represents the field mode operators and $\hat{\sigma}_m^{+/-}$ are the Pauli operators of the QD electron-hole pairs (excitons), ω_λ is the eigenfrequency corresponding to the transverse modes of the system $[\mathbf{f}_\lambda(\mathbf{r})]$, *excluding* the dots; $g_{m\lambda}$ is the field-dot coupling coefficient, defined through $g_{m\lambda} = \sqrt{\frac{\omega_\lambda}{2\hbar\varepsilon_0}} \boldsymbol{\mu}_m \cdot \mathbf{f}_\lambda(\mathbf{r}_m)$, with $\boldsymbol{\mu}_m = \mathbf{n}_m \mu_m$ the optical dipole moment of the QD electron-hole pair, aligned along $\mathbf{n}_m$ (a unit vector). Unless stated otherwise, we assume one target exciton in the spectral region of interest per QD with resonance frequency $\omega_{a/b}$. A schematic of the cavity-QD system is shown in Fig. 1.

The Heisenberg equations of motion for the operators can be used to derive the electric-field operator.[15,16] Subsequently, by assuming the weak excitation condition (i.e., we neglect higher order photon-correlation effects, which is valid in these systems for weak powers[17]), then the electric-field operator (ω is implicit)

$$\hat{\mathbf{E}}(\mathbf{r}) = \hat{\mathbf{E}}_0(\mathbf{r}) + \sum_{m=a,b} \frac{1}{\varepsilon_0} \underline{\mathbf{G}}^{(2)}(\mathbf{r},\mathbf{r}_m) \cdot \hat{\mathbf{d}}_m + \sum_{m=a,b} \underline{\mathbf{G}}^{(2)}(\mathbf{r},\mathbf{r}_m) \cdot \mathbf{n}_m \alpha_m \mathbf{n}_m \cdot \hat{\mathbf{E}}_0(\mathbf{r}_m), \tag{2}$$

where $\alpha_m(\omega) = \frac{\mu_m^2}{\hbar\varepsilon_0} \frac{2\omega_m}{\omega_m^2 - \omega^2 - i\omega\Gamma_m}$ is the dipole polarizability, with Γ_m the nonradiative decay rate, and

$$\hat{\mathbf{d}}_m = i\mu_m \left[\frac{\hat{\sigma}_m^-(t=0)}{\omega_m - \omega - i\Gamma_m/2} + \frac{\hat{\sigma}_m^+(t=0)}{\omega_m + \omega + i\Gamma_m/2} \right] \tag{3}$$

is a quantum *dipole source* that originates from the excited QDs. The propagator $\mathbf{G}^{(2)}(\mathbf{r},\mathbf{r}')$ is obtained from the Dyson equations,[16] and includes the contribution of two QDs through

$$\underline{\mathbf{G}}^{(2)}(\mathbf{r},\mathbf{r}_a) = \frac{\underline{\mathbf{G}}^{(1)}(\mathbf{r},\mathbf{r}_a) + \underline{\mathbf{G}}^{(1)}(\mathbf{r},\mathbf{r}_b) \cdot \mathbf{n}_b \alpha_b \mathbf{n}_b \cdot \underline{\mathbf{G}}^{(1)}(\mathbf{r}_b,\mathbf{r}_a)}{1 - \mathbf{n}_b \cdot \underline{\mathbf{G}}^{(1)}(\mathbf{r}_a,\mathbf{r}_b) \cdot \mathbf{n}_b \alpha_b \mathbf{n}_a \cdot \underline{\mathbf{G}}^{(1)}(\mathbf{r}_b,\mathbf{r}_a) \cdot \mathbf{n}_a \alpha_a}, \tag{4}$$

where

$$\underline{\mathbf{G}}^{(1)}(\mathbf{r},\mathbf{r}_m) = \frac{\underline{\mathbf{G}}(\mathbf{r},\mathbf{r}_m)}{1 - \mathbf{n}_m \cdot \underline{\mathbf{G}}(\mathbf{r}_m,\mathbf{r}_m) \cdot \mathbf{n}_m \alpha_m}. \tag{5}$$

With knowledge of the medium-dependent Green functions, and a suitable initial condition for exciting the material system, one can conveniently obtain the spectrum for two QDs, *in any medium*, from[18]

$$S(\mathbf{r},\omega) = \langle (\hat{\mathbf{E}}(\mathbf{r},\omega))^\dagger \hat{\mathbf{E}}(\mathbf{r},\omega) \rangle. \tag{6}$$

The exact quantum dynamics of two coupled QDs in cavity systems can also be solved using time-dependent integrodifferential equations, which, as might be expected, is also aided by using the Green function of the medium; for earlier work on two QD strong coupling effects in a semiconductor photonic crystal cavity, see Ref. 19.

We next apply the above general formalism to study the emitted spectrum of two excited QDs in a semiconductor micropillar system. The Green function of the elliptical cavity, with both x- and y-polarized modes, can be expressed via a simple Lorentzian decay model

$$\underline{\mathbf{G}}(\mathbf{r},\mathbf{r}') = \frac{\omega^2 \mathbf{f}_x(\mathbf{r}) \mathbf{f}_x^*(\mathbf{r}')}{\omega_x^2 - \omega^2 - i\omega\Gamma_x} + \frac{\omega^2 \mathbf{f}_y(\mathbf{r}) \mathbf{f}_y^*(\mathbf{r}')}{\omega_y^2 - \omega^2 - i\omega\Gamma_y}, \tag{7}$$

where for micropillar cavities emitting in the vertical direction, we can safely neglect the radiation-mode contribution.[17,18] Note that the $\mathbf{n}_x\mathbf{n}_x$ ($\mathbf{n}_y\mathbf{n}_y$) component of $\underline{\mathbf{G}}$ depends on the $\mathbf{f}_x$ ($\mathbf{f}_y$) field of the cavity mode. The cavity-QD coupling depends upon the projection of the dipole moment along the defined cavity axes x and y, e.g.,

$$\mathbf{n}_a \cdot \underline{\mathbf{G}}(\mathbf{r}_a,\mathbf{r}_a) \cdot \mathbf{n}_a \alpha_a = \frac{\mu_a^2}{\hbar\varepsilon_0} \frac{2\omega^2\omega_a}{\omega_a^2 - \omega^2 - i\omega\Gamma_a} \left[\frac{\mathbf{n}_a \cdot \mathbf{f}_x(\mathbf{r}) \mathbf{f}_x^*(\mathbf{r}') \cdot \mathbf{n}_a}{(\omega_x^2 - \omega^2 - i\omega\Gamma_x)} + \frac{\mathbf{n}_a \cdot \mathbf{f}_y(\mathbf{r}) \mathbf{f}_y^*(\mathbf{r}') \cdot \mathbf{n}_a}{(\omega_y^2 - \omega^2 - i\omega\Gamma_y)} \right], \tag{8}$$

which when coupled with Eqs. (2) and (6), fully describe both weak- and strong-coupling effects on an equal footing.

The emitted field from the cavity-QD system also depends upon the initial excitation conditions, typically achieved through steady-state pumping. It is shown in various other single QD-cavity systems, e.g., see Refs. 17, 20, and 21, that an appropriate excitation condition to consider is an *incoherently* excited system, where one has an effective exciton pump and cavity pump. In a Green function approach this condition is achieved by having the appropriate initial conditions for the various contributions to the electric-field operator, through

$$|\psi(t=0)\rangle = c_a|1\rangle_a|0\rangle_b|0\rangle_x|0\rangle_y + c_b|0\rangle_a|1\rangle_b|0\rangle_x|0\rangle_y + c_x|0\rangle_a|0\rangle_b|1\rangle_x|0\rangle_y + c_y|0\rangle_a|0\rangle_b|0\rangle_x|1\rangle_y, \tag{9}$$

where $|c_a|^2 + |c_b|^2 + |c_x|^2 + |c_y|^2 = 1$. The initial cavity field-

excited, for example, by the off-resonantly coupled QDs-is defined as

$$\hat{\mathbf{E}}_{0x/y}(\mathbf{r},\omega) = -\sqrt{\frac{\hbar\omega_{x/y}}{2\varepsilon_0}}\mathbf{f}_{x/y}(\mathbf{r})\hat{a}^0_{x/y}/(\omega_{x/y}-\omega-\Gamma_{x/y}/2) \quad (10)$$

while the initial exciton source depends on $\hat{\mathbf{d}}_m(\omega)$. Thus, for the example of no initial excitation of the cavity modes, and considering only one incoherently excited QD, we recover earlier Green function results.[18] In addition, for any incoherent excitation conditions, we emphasize that this approach formally recovers results from a master-equation approach,[17,20,21] if working in the weak excitation regime. However, a clear advantage of the present approach is that any generalized excitation can be considered, including coherent Bell states,[16] and, as long as one can obtain $\underline{\mathbf{G}}$, the QD coupling can also be explored in any generalized medium, including coupled cavity[22] and coupled cavity waveguide systems,[23] which are ill-suited problems for quasi-Markovian master-equation techniques.

Briefly summarizing this section, we have obtained an *analytical* solution for the emitted spectrum that allows one to perform parameter sweeps in a straightforward and physically intuitive way. Using the analytical form for the cavity-mode Green function, we are in effect computing the cavity emitted spectrum, which is known to be the dominant decay channel in these systems; the generalization to include radiation-mode decay via the QD (spontaneous) emission is simple.[18] In what follows below, we will neglect any initial coherence in the system and consider only an *incoherent* excitation. While this initial condition can certainly be generalized, we find an excellent qualitative agreement with the experiments.

III. EXPERIMENTAL POLARIZATION-DEPENDENT PHOTOLUMINESCENCE AND COMPARISON WITH THEORY

Our experiments were performed on high-quality QD micropillars based on a planar AlAs/GaAs microcavity structure. The micropillars contain a low-density ($n_{QD} \approx 5 \times 10^9$ cm^{-2}) layer of large elongated $In_{0.3}Ga_{0.7}As$ QDs in the active region and were realized by high-resolution electron-beam lithography and electron cyclotron resonance plasma etching (see also the schematic in Fig. 1). For details on the fabrication process we refer to Ref. 24. The micropillars were investigated under nonresonant (532 nm or 3.33 eV) cw excitation at low temperature (5–40 K) using a high-resolution microphotoluminescence (μPL) setup with a spectral resolution of 16 μeV.[25] A linear polarizer was installed in the photoluminescence detection path in order to measure polarization-resolved μPL spectra.

Figure 2(a) shows μPL spectra of a micropillar with $d = 1.6$ μm for 0° and 90° (linear x and y, respectfully) detection angle at 24 K. As a consequence of a slight ellipticity of the pillar cross section the twofold degeneracy of the fundamental mode is lifted and two orthogonal linearly polarized components (Γ_x and Γ_y) split by $\Delta E_{xy} \approx 170$ μeV are observed. The spectral splitting ΔE_{xy} between the two mode components is associated with an ellipticity $\epsilon = (\alpha/\beta)^{0.5} - 1$ of

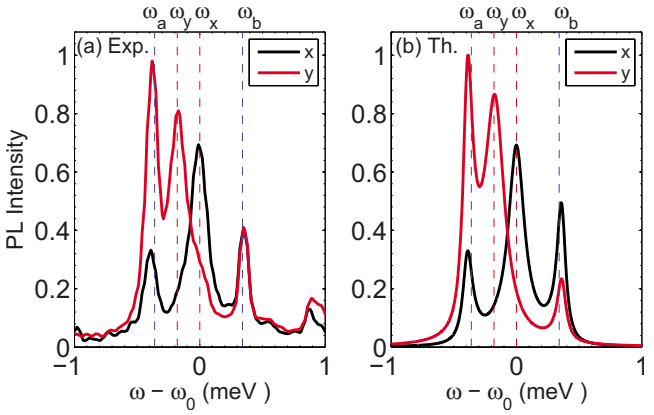

FIG. 2. (Color online) (a) Experimental μPL spectra for a 1.6 μm diameter micropillar with slightly elliptical cross section under x and y detection angles at 24 K. The fundamental cavity mode is split by around 170 μeV into two linearly polarized components near ω_x and ω_y. The QD excitons X_a (ω_a) and X_b (ω_b) can be tuned through resonance with cavity modes by means of temperature detuning. The labeling of ω_0 in the detuning is just for convenience and in this case $\omega_0 \approx 1.326$ eV. (b) Corresponding calculation for a two QD-cavity system, assumed to be aligned at $\pi/4$ with respect to the x and y axis, with $g = 100$ μeV, $\Gamma_x = 160$ μeV, $\Gamma_y = 200$ μeV, and $\Gamma_a = \Gamma_b = 80$ μeV. The example initial pump conditions correspond to $c_a = c_b$, $c_x = 0.33c_a$, and $c_y = 0.5c_a$.

about 0.005, where α (β) denotes the long (short) axis of the elliptical cross section of the pillar.[25] From Lorentzian line-shape fitting we determined Q factors of 8300 ($\Gamma_x = 160$ μeV) for the high-energy component at 0° and 6700 ($\Gamma_y = 200$ μeV) for the low-energy component at 90°. Two exciton lines labeled as X_a and X_b are observed close to the cavity mode and can be shifted into resonance with Γ_x and Γ_y by temperature tuning. The two exciton lines are not coupled electronically but there exists an indirect coupling via a photon exchange that is mediated by the common cavity mode. Since the exciton lines are spectrally separated by an energy (750 μeV) that significantly exceeds the cavity-mode linewidths, the photon mediated coupling can be considered as incoherent in contrast to the coherent coupling of two separate QDs reported in Ref. 7.

The coupling behavior of the QD-micropillar system was investigated for 0° (x polarization) and 90° (y polarization), respectively, by measuring temperature dependent μPL spectra (not shown). We applied Lorentzian line-shape fitting of the four involved modes ($\Gamma_x, \Gamma_y, X_a, X_b$) to extract the corresponding energies as a function of temperature. In this temperature dependence we observe anticrossings of excitons X_a and X_b with both linearly polarized components of the split fundamental mode of the micropillar. Due to the different emission energies of the Γ_x and Γ_y components, resonance is achieved at different temperatures with a higher resonance temperature for the low energetic component Γ_y. In particular, X_a (X_b) is in resonance with Γ_x at 11 K (31 K), whereas resonance with Γ_y is observed at about 18 K (34 K). Here, the individual splitting in resonance, i.e., the vacuum Rabi splitting, depends, via $\Delta E_R = 2\sqrt{g^2 - (\Gamma_{x/y} - \Gamma_{a/b})^2/4}$, not only on the coupling constant of exciton g_a/g_b but also on the linewidth of the cavity component $\Gamma_{x/y}$ (neglecting the influ-

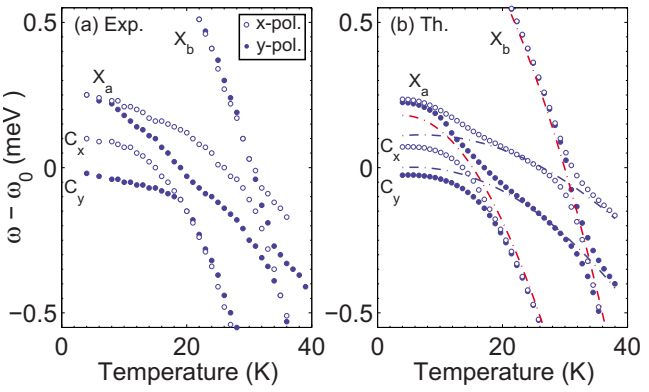

FIG. 3. (Color online) (a) Experimental energy dispersion of the excitonic (X_a, X_b) and photonic (Γ_x, Γ_y) emission under x and y detection angle. (b) Theoretical dispersion graphs using similar parameters to those employed in Fig. 2. The emission energies of the uncoupled modes are indicated by chain lines. Note that since we constrain all the parameters to achieve a reasonable fit over all temperatures, but we have slightly adjusted the global linewidths, and reduced the g by 10%, which helps to ensure that a true peak is identified in the spectra for all temperatures (Ref. 27).

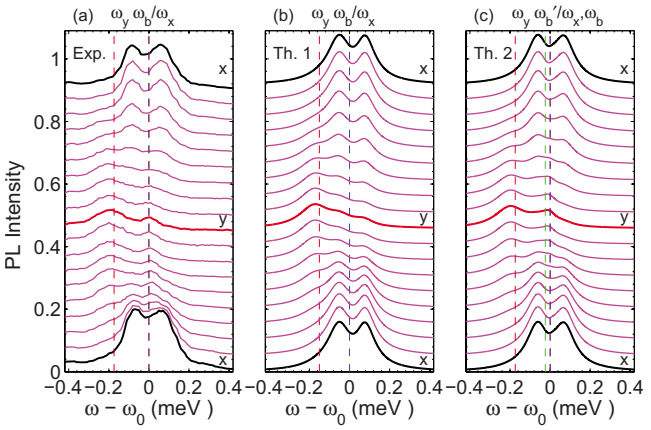

FIG. 4. (Color online) (a) μPL emission spectra at 31 K under variation in the detector angle between x through an angle of π radians (x to y to x). At y detection angle, the emission from ω_y and ω_b is detected. (b) Calculation using identical parameters to Fig. 1 but for one coupled X only (X_b), and with different initial conditions: $c_b = 1.18c_a$, $c_x = 1.06c_b$, $c_y = 0.76c_a$. (c) Now we add in a perpendicular dipole aligned at $-\pi/4$ (45°) with $d_{b'} = d_b/3$ (see text), which is expected for our elongated dots (Ref. 28), and yields a center peak in better agreement with the experiments.

ence of $\Gamma_{a/b} \ll \Gamma_{x/y}$). In fact, the lower linewidth $\Gamma_x = 160$ μeV of the Γ_x component results in a larger ΔE_R of 140 μeV (135 μeV) for X_a (X_b) in comparison with the vacuum Rabi splitting of 115 μeV (120 μeV) for X_a (X_b) observed for the Γ_y component with a linewidth of 200 μeV.

In Fig. 2(b) we show the corresponding theoretical calculation. Good qualitative agreement between experiment [Fig. 2(a)] and theory [Fig. 2(b)] is obtained for $g = 100$ μeV and $\Gamma_x = 160$ μeV, $\Gamma_y = 200$ μeV, as well as $\Gamma_a = \Gamma_b = 80$ μeV which are determined from experiment. The initial pump conditions are $c_a = c_b$, $c_x = 0.33c_a$, and $c_y = 0.5c_a$. Since there are clearly other excitons involved in the coupling regime [e.g., near +0.9 meV, Fig. 2(a)], we have not tried to obtain a best fit, but rather just chose an example that produces the same qualitative trend as in the experiments, while constraining as much approximately known parameters as possible. The elongated $In_{0.3}Ga_{0.7}As$ QDs with typical lengths of 50–100 nm and widths of about 30 nm before overgrowth are aligned preferentially orientated along the $[0\bar{1}1]$ direction,[26] which is at 45° with respect to the minor and major axis of the micropillar cavity. Therefore, in the calculations, the two QDs were aligned in 45° orientation with respect to the x and y axes. Note that in both experiment and theory, a pronounced polarization dependence with stronger emission in y direction is observed for X_a which is attributed to light-matter coupling between X_a and the spectrally close y component of the cavity mode.

Having understood the basic light-matter interaction of two QDs coupled to two orthogonal cavity modes, we are now in a position to study the polarization-resolved coupling behavior in more detail. For this purpose, the energy dispersions of the interaction modes are calculated for polarization directions x and y as a function of temperature. The results are plotted in Fig. 3(b) along with the experimental data in panel (a). As a guide to the eye, the dispersions of the uncoupled modes are indicated as chain lines. Again a good qualitative agreement between experiment and theory is obvious: X_a shows anticrossing and resonance with the Γ_x component at about 10 K. Coherent interaction with the Γ_y mode is observed at 18 K. For higher temperatures, X_b is clearly interacting with Γ_x at 31 K and Γ_y at 34 K, respectively.

To further investigate the polarization dependence of the exciton-photon interaction, polarization resolved measurements were performed at fixed temperature $T = 31$ K when X_2 is on resonance with Γ_x while a detuning of 180 μeV is achieved between X_2 and the orthogonal component Γ_y. The corresponding spectra are plotted in Fig. 4(a) for detection angles between 0° and 180°. At detection angles of 0° and 180° the double-peak emission feature clearly reflects the coherent coupling between Γ_x and X_b. In contrast, at 90° detection, the cavity mode Γ_x is seen and another single emission peak appears at $w - w_0 = 0$. The latter is associated with emission from an uncoupled component of X_b. In fact, it is nicely seen that the X_b emission at 90° coincides spectrally with w_0 as expected for zero detuning. In panel (b) the corresponding theoretical simulation is shown for interaction between X_b and Γ_x, Γ_y, using identical linewidths and coupling constant to Fig. 2 but with slightly different initial conditions: $c_b = 1.18c_a$, $c_x = 1.06c_b$, $c_y = 0.76c_a$. While the characteristic double peak for strong coupling is nicely reproduced by theory at 0° and 180° detection angle, the experimental and theoretical spectra deviate clearly at 90° (y-polarization detection), where the double-peak feature is maintained also at 90° in case for the calculated spectra. This discrepancy is attributed to the fact that so far we have considered only one dipole, with a dipole moment d_b aligned along the axis of the elongated QD. As a consequence, the exciton couples with equal strength to the Γ_x and Γ_y mode and the double-peak feature appears at 90°. By adding a perpendicular dipole with a dipole moment $d_{b'} = d_b/3$ we ob-

tain the spectra depicted in Fig. 3(c) which, obviously, are in much better agreement with the experimental data. In fact, a small perpendicular dipole moment is expected for our elongated QDs.[28] It is interesting to mention that the dipole moment of a strongly coupled QD has an orientation that is well aligned with the coupled cavity mode, whereby the possible effect of the fine-structure is insignificant.[29] We further note that at the x and y detection angle the effect of this smaller perpendicular dipole (per QD) is negligible, thus justifying the two dipole model used in Figs. 2 and 3. Moreover, we have repeated the simulations in Figs. 2 and 3 with two dipoles per QD and find only a minor quantitative difference when the additional dipole is added; so the influence of a possible perpendicular dipole is only observed by measuring the full polarization properties of the emission.

IV. CONCLUSION

We have presented both experimental measurements and the theory of polarization-dependent strong-coupling regime in elliptical high-Q micropillar cavity. Our results are important for understanding the fundamental light-matter interactions in these semiconductor cavity systems and form an important prerequisite for exploit such interactions in next generation to quantum optical devices, such as the cavity-assisted creation of polarization-entangled photon pairs.[13,14]

ACKNOWLEDGMENTS

The authors would like to thank M. Emmerling and A. Wolf for expert sample preparation. This work was supported by the Deutsche Forschungsgemeinschaft via the Research Group "Quantum Optics in Semiconductor Nanostructures," the European Commission through the Project "QUANTIP," the State of Bavaria, the National Sciences and Engineering Research Council of Canada, and the Canadian Foundation for Innovation.

*stephan.reitzenstein@physik.uni-wuerzburg.de

[1] J. P. Reithmaier, G. Sek, A. Löffler, C. Hofmann, S. Kuhn, S. Reitzenstein, L. V. Keldysh, V. D. Kulakovskii, T. L. Reinecke, and A. Forchel, Nature (London) **432**, 197 (2004).

[2] T. Yoshie, A. Scherer, J. Hendrickson, G. Khitrova, H. M. Gibbs, G. Rupper, C. Ell, O. B. Shchekin, and D. G. Deppe, Nature (London) **432**, 200 (2004).

[3] D. Press, S. Götzinger, S. Reitzenstein, C. Hofmann, A. Löffler, M. Kamp, A. Forchel, and Y. Yamamoto, Phys. Rev. Lett. **98**, 117402 (2007).

[4] K. Hennessy, A. Badolato, M. Winger, D. Gerace, M. Atatüre, S. Gulde, S. Fält, E. L. Hu, and A. Imamoğlu, Nature (London) **445**, 896 (2007).

[5] A. Faraon, I. Fushman, D. Englund, N. Stoltz, P. Petroff, and J. Vučković, Nat. Phys. **4**, 859 (2008).

[6] J. Kasprzak, S. Reitzenstein, E. A. Muljarov, C. Kistner, C. Schneider, M. Strauss, S. Höfling, A. Forchel, and W. Langbein, Nature Mater. **9**, 304 (2010).

[7] S. Reitzenstein, A. Löffler, C. Hofmann, A. Kubanek, M. Kamp, J. P. Reithmaier, A. Forchel, V. D. Kulakovskii, L. V. Keldysh, I. V. Ponomarev, and T. L. Reinecke, Opt. Lett. **31**, 1738 (2006).

[8] C. Kistner, T. Heindel, C. Schneider, A. Rahimi-Iman, S. Reitzenstein, S. Höfling, and A. Forchel, Opt. Express **16**, 15006 (2008).

[9] A. Laucht, F. Hofbauer, N. Hauke, J. Angele, S. Stobbe, M. Kaniber, G. Böhm, P. Lodahl, M.-C. Amann, and J.-J. Finley, New J. Phys. **11**, 023034 (2009).

[10] C. Kistner, K. Morgener, S. Reitzenstein, C. Schneider, S. Höfling, L. Worschech, and A. Forchel, Appl. Phys. Lett. **96**, 221102 (2010).

[11] M. Winger, A. Badolato, K. J. Hennessy, E. L. Hu, and A. Imamoğlu, Phys. Rev. Lett. **101**, 226808 (2008).

[12] S. Reitzenstein, S. Münch, P. Franeck, A. Löffler, S. Höfling, L. Worschech, A. Forchel, I. V. Ponomarev, and T. L. Reinecke, Phys. Rev. B **82**, 121306(R) (2010).

[13] R. Johne, N. A. Gippius, G. Pavlovic, D. D. Solnyshkov, I. A. Shelykh, and G. Malpuech, Phys. Rev. Lett. **100**, 240404 (2008).

[14] P. K. Pathak and S. Hughes, Phys. Rev. B **79**, 205416 (2009).

[15] M. Wubs, L. G. Suttorp, and A. Lagendijk, Phys. Rev. A **70**, 053823 (2004).

[16] P. Yao and S. Hughes, Opt. Express **17**, 11505 (2009).

[17] P. Yao, P. K. Pathak, E. Illes, S. Hughes, S. Münch, S. Reitzenstein, P. Franeck, A. Löffler, T. Heindel, S. Höfling, L. Worschech, and A. Forchel, Phys. Rev. B **81**, 033309 (2010).

[18] S. Hughes and P. Yao, Opt. Express **17**, 3322 (2009).

[19] S. Hughes, Phys. Rev. Lett. **94**, 227402 (2005).

[20] F. P. Laussy, E. del Valle, and C. Tejedor, Phys. Rev. Lett. **101**, 083601 (2008).

[21] A. Laucht, N. Hauke, J. M. Villas-Bôas, F. Hofbauer, M. Kaniber, G. Böhm, and J. J. Finley, Phys. Rev. Lett. **103**, 087405 (2009).

[22] S. Hughes, Phys. Rev. Lett. **98**, 083603 (2007).

[23] S. Hughes and H. Kamada, Phys. Rev. B **70**, 195313 (2004); see also E. Waks and J. Vučković, Phys. Rev. Lett. **96**, 153601 (2006).

[24] S. Reitzenstein and A. Forchel, J. Phys. D: Appl. Phys. **43**, 033001 (2010).

[25] S. Reitzenstein, C. Hofmann, A. Gorbunov, M. Strauß, S. H. Kwon, C. Schneider, A. Löffler, S. Höfling, M. Kamp, and A. Forchel, Appl. Phys. Lett. **90**, 251109 (2007).

[26] A. Löffler, J.-P. Reithmaier, A. Forchel, A. Sauerwald, D. Peskes, T. Kümmell, and G. Bacher, J. Cryst. Growth **286**, 6 (2006).

[27] In fact, it is known that g can change as a function of temperature-detuning because of electron-phonon scattering (Refs. 30–32), so it is reasonable to slightly change this for the best global fit.

[28] See, for example, A. Muller, Q. Q. Wang, P. Bianucci, C. K. Shih, and Q. K. Xue, Appl. Phys. Lett. **84**, 981 (2004), where the authors' note: "we find that the ratio of the two dipole moments is close to the physical elongation ratio of the quantum

dot"—which perfectly corresponds with our assumptions for Fig. 4(c).

[29] We would like to point out that the fine-structure splitting is not particularly large for the elongated $In_{0.3}Ga_{0.7}As$ QDs. A statistical analysis such QDs revealed an average fine-structure splitting of 5 μeV. This is consistent with the interpretation that the excitons are weakly confined in these large QDs.

[30] I. Wilson-Rae and A. Imamoğlu, Phys. Rev. B **65**, 235311 (2002).

[31] F. Milde, A. Knorr, and S. Hughes, Phys. Rev. B **78**, 035330 (2008).

[32] P. Kaer, T. R. Nielsen, P. Lodahl, A.-P. Jauho, and J. Mørk, Phys. Rev. Lett. **104**, 157401 (2010).